Algorithm Technical Background Document

The MODIS Near-IR Water Vapor Algorithm

Product ID: MOD05 - **Total Precipitable Water**

Bo-Cai Gao[1] and Yoram J. Kaufman[2]

[1]Remote Sensing Division, Code 7212, Naval Research Laboratory
4555 Overlook Avenue, SW, Washington, DC 20375

[2]Climate and Radiation Branch, NASA Goddard Space Flight Center
Greenbelt, MD 20771

TABLE OF CONTENTS

Summary

The MODIS Near-Infrared Total Precipitable Water Product (MOD 05) consists of column water vapor amounts over clear land areas of the globe, and above clouds over both land and ocean. Water vapor estimates are also made over extended oceanic areas with Sun glint. The retrieval algorithm relies on observations of water vapor attenuation of near-IR solar radiation reflected by surfaces and clouds. The product is produced only over areas that have reflective surfaces in the near-IR. Techniques employing ratios of water vapor absorbing channels centered near 0.905, 0.936, and 0.94 μm with atmospheric window channels at 0.865 and 1.24 μm are used. The ratios partially remove the effects of variation of surface reflectance with wavelengths and result in the atmospheric water vapor transmittances. The column water vapor amounts are derived from the transmittances based on theoretical radiative transfer calculations and using look-up table procedures. Experience in this retrieval has been gained through analysis of spectral imaging data acquired with the Airborne Visible Infrared Imaging Spectrometer (AVIRIS) aboard an ER-2 aircraft. Water vapor values can be determined with errors typically in the range between 5% and 10%. The errors will be greater for retrievals from data collected over dark surfaces or under hazy conditions. A module for correcting aerosol effects has been developed and implemented in the MODIS near-IR water vapor algorithm. A quality control parameter will be used to indicate the reliability of the retrieval.

Both daily Level 2 (MOD05) and daily, 8-day, and monthly Level 3 (MOD43) gridded products will be produced. The Level 2 data are generated at the 1-km spatial resolution of the MODIS instrument; Level 3 data are computed on 0.5° latitude and longitude, equal area and equal angle grids. These products are essential to the understanding of the hydrological cycle, aerosol properties, aerosol-cloud interactions, energy budget, and climate. Of particular interest is the collection of water vapor data above cirrus clouds over water surfaces, which has important applications to climate studies.

1 Introduction

This document is a description of the algorithm for deriving column water vapor amounts from measurements of near-IR solar radiation reflected by the land surface (or by clouds) with the Moderate Resolution Imaging Spectrometer (MODIS) (Salomonson et al., 1989; King et al., 1992) on the Earth Observing System (EOS) Polar Platform. MODIS channels centered at 0.865, 0.905, 0.936, 0.940, and 1.24 μm are used. Techniques employing ratios of water vapor absorbing channels at 0.905, 0.936, and 0.94 μm with atmospheric window channels at 0.865 and 1.24 μm are used. The ratios partially remove the effects of variation of surface reflectances with wavelengths and give approximately the atmospheric water vapor transmittances. The column water vapor amounts are derived from the transmittances based on theoretical radiative transfer calculations and using look-up table procedures.

Background information on deriving column water vapor from near-IR channels is described in Section 2. The information was previously described by Kaufman and Gao (1992), and Gao and Goetz (1990). Detailed description of the algorithm is presented in Section 3. Calibration, validation, and quality assurance plans are given in Section 4. Research agenda are described in Section 5.

2 Overview and Background Information

The objective of this algorithm, the historical perspective on derivation of water vapor values from satellite measurements, and the unique features of near-IR MODIS channels, are described in this section.

2.1 Experimental Objective

The purpose of this algorithm is to derive column water vapor amounts over clear land areas of the globe, above clouds over both land and ocean, and over extended oceanic areas with Sun glint. The derivation will be made separately over cloud free pixels and over cloudy pixels. The data product is important to increase our understanding of the hydrological cycle, aerosol properties, aerosol-cloud interactions, energy budget, and climate.

2.2 Historical Perspective

Historically, remote sensing of water vapor profiles from space was made using IR emission channels. The results depended in part on the initial guess for the

temperature and moisture profiles used in the inversion (Susskind et al., 1984). Column water vapor amounts over the ocean were retrieved from IR emission channels in the 11 - 13 μm spectral region using "split window" techniques (Chesters et al., 1983) and from microwave emission measurements. The "split window" techniques also work well over land areas covered by green vegetation. When the apparent surface temperature, which is the product of surface emissivity and skin temperature, is about equal to the average temperature of the boundary layer, where most of the water vapor usually resides, infrared and microwave remote sensing will not be sensitive to the boundary layer water vapor.

MODIS is an instrument that has near-IR channels within and around the 0.94-μm water vapor band for remote sensing of column water vapor amounts over the globe from a satellite platform. Over the past few years, experience (Gao and Goetz, 1990; Gao et al., 1993) has been gained in deriving column water vapor amounts from the 0.94-μm water vapor band using data acquired with the JPL Airborne Visible Infrared Imaging Spectrometer (AVIRIS) (Vane et al., 1993) from a NASA ER-2 aircraft platform.

2.3 Instrument Characteristics

MODIS is a major facility instrument on the EOS polar orbiting satellite platforms (Asrar and Greenstone, 1995; King et al., 1992; Salomonson et al., 1989) designed to measure biological and physical processes on a global scale every 1 to 2 days. It is a 36-channel scanning radiometer covering the spectral region 0.4 - 15 μm. Five near-IR MODIS channels are useful for remote sensing of water vapor. The positions and widths of these channels are given in Table 1 and illustrated in Figure 1. Two atmospheric water vapor transmittance spectra for the Tropical and Sub-Arctic Winter Models in LOWTRAN7 (Kneizys et al., 1988) with a solar zenith angle of 45 degrees and a nadir-looking geometry are also shown in Figure 1. The channels at 0.865 and 1.24 μm are non-absorption channels present on MODIS for remote sensing of vegetation and clouds. The channels at 0.935, 0.940, and 0.905 μm are water vapor absorption channels with decreasing absorption coefficients. The strong absorption channel at 0.935 μm is most useful for dry conditions, while the weak absorption channel at 0.905 μm is most useful for very humid conditions, or low solar elevation.

Table 1: Positions and widths of five MODIS near-IR channels used in water vapor retrievals.

MODIS Channel #	Position (μm)	Width (μm)
2	0.865	0.040
5	1.240	0.020
17	0.905	0.030
18	0.936	0.010
19	0.940	0.050

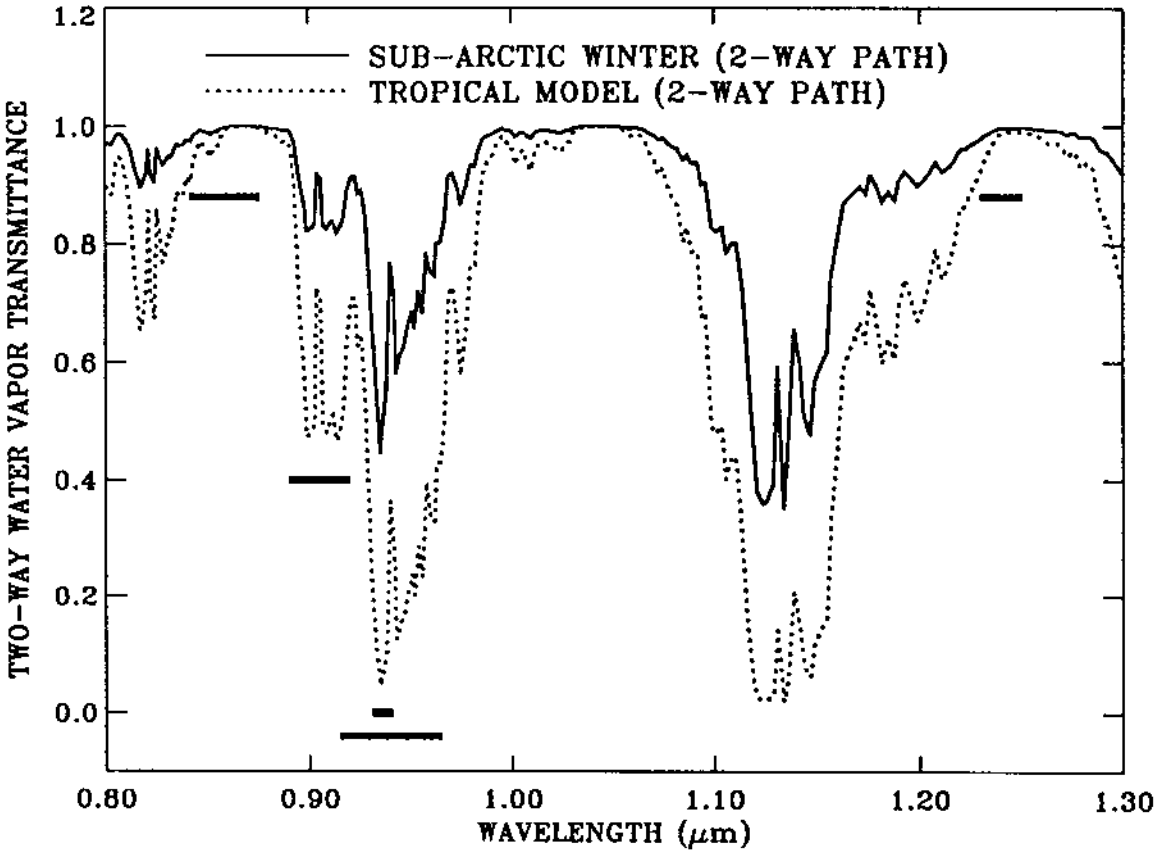

Fig. 1. Positions and widths of five MODIS near-IR channels marked in thick horizontal bars, and 2-way atmospheric water vapor transmittance spectra for Tropical and Sub-Arctic Winter Models in LOWTRAN7 (Kneizys et al., 1988) with a solar zenith angle of 45 degrees and a nadir-looking geometry.

3 Algorithm Description

Our algorithm for deriving column water vapor amounts from near-IR channels on MODIS is described from both theoretical and practical point of view in this section.

3.1 Theoretical Description

3.1.1 Physics of the Problem

The remote sensing method is based on detecting the absorption by water vapor of the reflected solar radiation after it has transferred down to the surface and back up through the atmosphere. The total vertical amount of water vapor can be derived from a comparison between the reflected solar radiation in the absorption channel, and the reflected solar radiation in nearby non-absorption channels. Detailed descriptions of the remote sensing method have been published (Kaufman and Gao, 1992; Gao and Goetz, 1990) and are enclosed in Appendices A and B. Below are abbreviated descriptions of the remote sensing method. General descriptions of remote sensing of cloud, aerosol, and water vapor properties from MODIS have been given by King et al. (1992).

The solar radiation between 0.86 and 1.24 μm on the Sun-surface-sensor path is subjected to atmospheric water vapor absorption, atmospheric aerosol scattering, and surface reflection. In order to derive column water vapor from measurements of solar radiation reflected by the surface, the absorption and scattering properties of the atmosphere and the surface near 1 μm must be taken into consideration.

Atmospheric Absorption and Scattering in the 0.86-1.24 μm Range

The radiance at a downward-looking satellite sensor can be written (Hansen and Travis, 1974, Fraser and Kaufman, 1985), in a simplified form, as

$$L_{Sensor}(\lambda) = L_{Sun}(\lambda)\, T(\lambda)\, \rho(\lambda) + L_{Path}(\lambda) \qquad (1)$$

where λ is the wavelength, $L_{Sensor}(\lambda)$ is the radiance at the sensor, $L_{Sun}(\lambda)$ is the solar radiance above the atmosphere, $T(\lambda)$ is the total atmospheric transmittance, which is equal to the product of the atmospheric transmittance from the Sun to the Earth's surface and that from the surface to the satellite sensor, $\rho(\lambda)$ is the surface bi-

directional reflectance, and $L_{Path}(\lambda)$ is the path scattered radiance. Eq. (1) is simplified in a sense that photons that are reflected from the surface more than once are being ignored. This feedback mechanism involves back scattering to the surface by the atmosphere. The feedback effect is usually small, because aerosol optical thicknesses are typically small in the near-IR region. The first term on the right side of Eq. (1) is the direct reflected solar radiation. L_{Direct} is used to represent this component. $L_{Sensor}(\lambda)/L_{Sun}(\lambda)$ is defined as the apparent reflectance $\rho^{*}(\lambda)$ in this document.

The $T(\lambda)$ contains information about the total amount of water vapor in the combined Sun-surface-sensor path. $L_{Sun}(\lambda)$ is a known quantity. Near 1 μm, Rayleigh scattering is negligible and the main contribution to $L_{Path}(\lambda)$ is scattering by aerosols. $L_{Path}(\lambda)$ in the 1 μm region is usually a few percent of the direct reflected solar radiation. Because most aerosols are located in the lower 2 km of the atmosphere and the same is true for atmospheric water vapor, the single and multiple scattered radiation by aerosols is also subjected to water vapor absorption. As a result, $L_{Path}(\lambda)$ contains water vapor absorption features (Gao and Goetz, 1990). We assume that $L_{Path}(\lambda)$ can be treated approximately as an unspecified fraction of direct reflected solar radiation when the aerosol concentrations are low. This assumption allows the derivation of column water vapor amounts from satellite data without the need to model single and multiple scattering effects. In the following we describe in detail the water vapor retrieval algorithm for cloud free pixels. A similar algorithm is applicable for retrievals over cloudy pixels.

Surface Reflectances Near 1 μm

Most land is either covered by soils, rocks, vegetation, snow, or ice. Figure 2 shows reflectance curves of five major types of soil (Condit, 1970; Stoner and Baumgardner, 1980). The reflectances between 0.85 and 1.25 μm change approximately linearly with wavelength. Similar linearity is observed in reflectance spectra of common rocks and minerals. The largest deviation from linearity is observed in reflectance spectra of iron-rich soils and minerals. These materials have broad electronic bands, which are related to the Fe^{3+} transition and are centered near 0.86 μm. Curve 3 in Fig. 2 shows such a broad band feature in the spectral region between approximately 0.8 and 1.25 μm.

Figure 3 shows vegetation and snow reflectance spectra (Bowker et al., 1985). The vegetation spectrum has liquid water bands centered at approximately 0.98 and

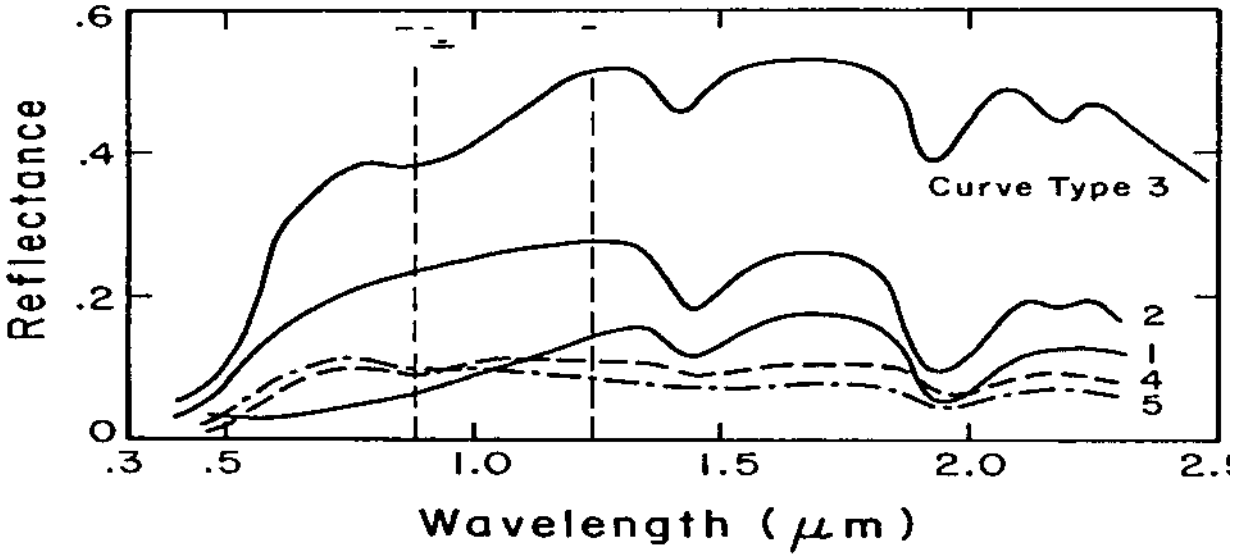

Fig. 2. Typical soil reflectance curves for five major soil types [*Condit, 1970; Stoner and Baumgartner,* 1980]: (1) organic-dominated, moderately fine texture; (2) organic-affected, moderately course texture; (3) iron dominated laterite-type soil; (4,5) iron- and organic-rich soil, respectively.

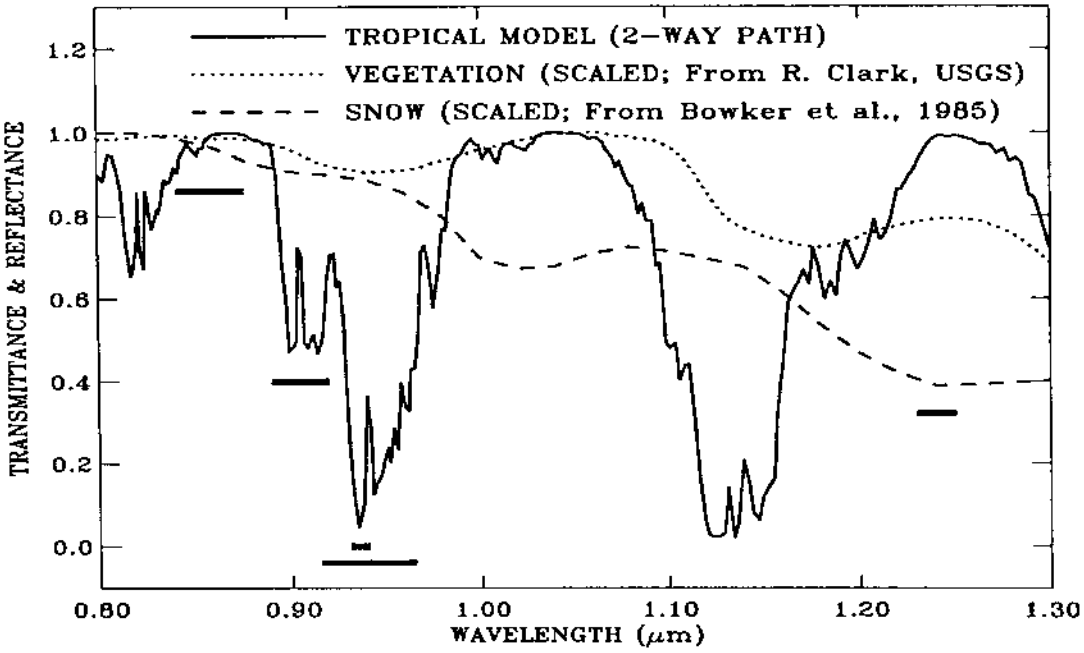

Fig. 3. A 2-way transmittance spectrum of atmospheric water vapor and reflectance spectra (scaled) of vegetation and snow. The band centers of water vapor, liquid water and ice are relatively shifted by approximately 50 nm.

1.20 μm. The snow spectrum has ice absorption bands centered approximately at 1.04 and 1.24 μm. For comparison, Fig. 3 also shows a calculated water vapor transmittance spectrum. The positions of water vapor, liquid water and ice absorption bands are shifted relative to each other. The shifting of the vibrational bands is due to increases in intermolecular forces as the water molecules become more organized in the liquid and solid states.

Transmittance Derivation Using Channel Ratioing Techniques

The reflectance values at a given wavelength are quite different for different types of surfaces, as seen from Figures 2 and 3. It is not possible to get the water vapor transmittances (see Eq. (1)) from radiances of individual absorption channels. However, if the surface reflectances are constant with wavelength, a 2-channel ratio of an absorption channel with a window channel gives the water vapor transmittance of the absorption channel. For example, the transmittance of the channel at 0.94 μm

$$T_{obs}(0.94\ \mu m) = \rho^{*}(0.94\ \mu m)\ /\ \rho^{*}(0.865\ \mu m) \qquad (2)$$

if the surface reflectances are constant with wavelength and if the path radiances can be treated as small fractions of directly reflected solar radiances.

If surface reflectances vary linearly with wavelength, a 3-channel ratio of an absorption channel with a combination of two window channels gives the water vapor transmittance of the absorption channel. For example, the transmittance of the channel at 0.94 μm

$$T_{obs}(0.94\ \mu m) = \rho^{*}(0.94\ \mu m)\ /\ [C_1 * \rho^{*}(0.865\ \mu m) + C_2 * \rho^{*}(1.24\ \mu m)], \qquad (3)$$

where C_1 is equal to 0.8, and C_2 0.2.

Water Vapor Retrievals Over Land And Oceanic Areas With Sun Glint

Both the 2-channel and 3-channel ratioing techniques will be used to derive atmospheric transmittances of the absorption channels, and subsequently the column water vapor amounts over clear land areas and extended oceanic areas with sun glint. The 2-channel and 3-channel ratios will be calculated from radiances of the five MODIS channels centered at 0.865, 0.905, 0.936, 0.94, and 1.24 μm. These channel ratios are approximately equal to the atmospheric water vapor

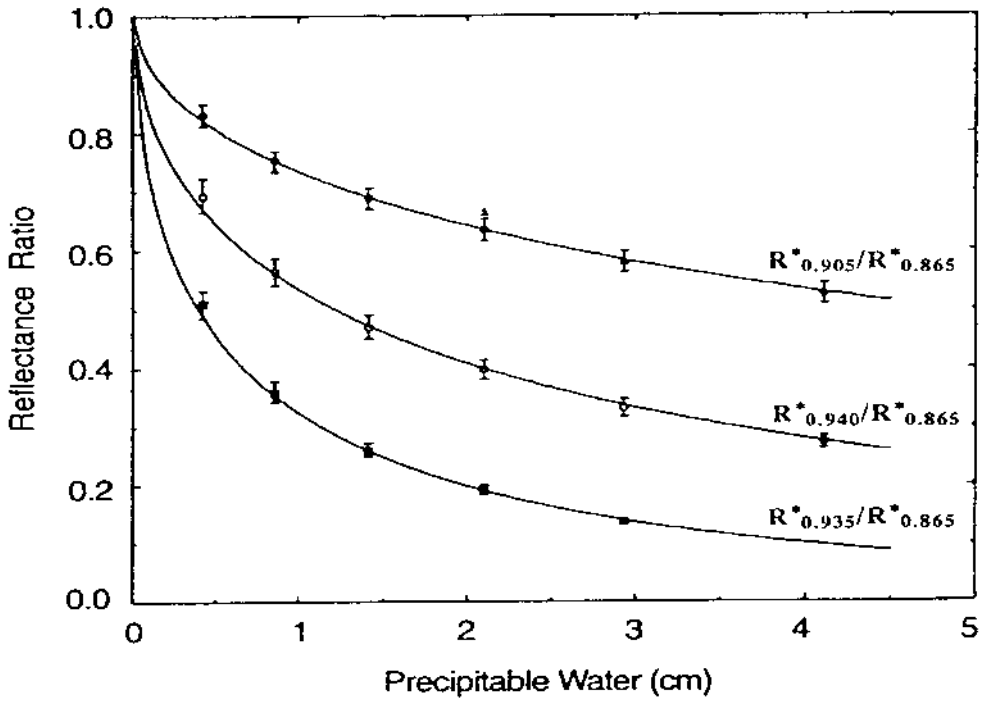

Fig. 4. The dependence of the reflectance ratio, defined as the ratio between the apparent reflectance in a water vapor absorbing channel and the radiance in the nonabsorbing channel around 0.865 μm, on the amount of water vapor in a vertical column (Kaufman and Gao, 1992).

transmittances in the Sun-surface-sensor ray path. Look-up tables containing values of 2-channel and 3-channel ratios and total amounts of water vapor are generated using radiative transfer programs, such as LOWTRAN7 (Kneizys et al., 1988), MODTRAN, or a line-by-line code. Figure 4 shows examples of 2-channel ratios (absorption channel / window channel) as a function of column water vapor amount. The total amount of water vapor in the 2-way path is derived from values of 2-channel and 3-channel ratios calculated from the MODIS data using a table-searching procedure. The derived total water vapor amount is then converted to the column water vapor amount based on the solar and the observational geometries. Our sensitivity studies show that a 0.01 error in derived transmittance using channel ratio techniques gives roughly 2.5% error in the retrieved column water vapor amounts.

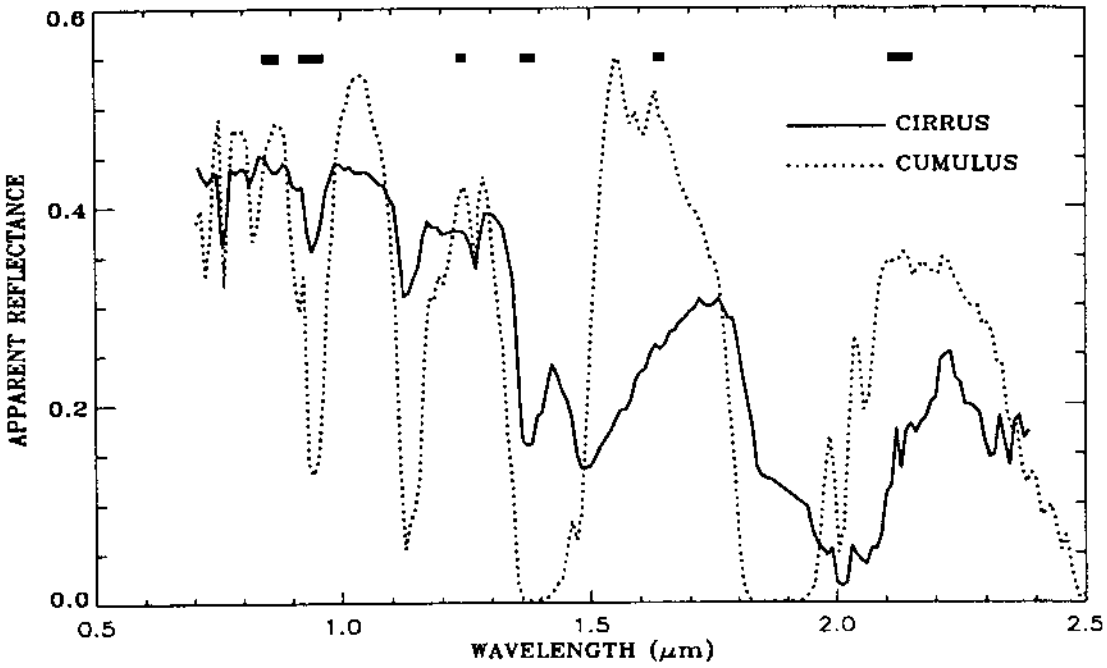

Fig. 5. Sample cumulus and cirrus cloud spectra over water surfaces measured with the NASA/JPL Airborne Visible Infrared Imaging Spectrometer from an ER-2 aircraft at 20 km. Because cirrus clouds are much higher than cumulus clouds, the peak absorption feature of the 0.94-μm water vapor band for the cirrus spectrum is much smaller than that for the cumulus spectrum.

Water Vapor Retrievals Over Clouds

When clouds are present, the MODIS channels in the 0.8 - 2.5 μm region contain information about absorptions due to water vapor above and within clouds. This is illustrated in Figure 5, in which sample cumulus and cirrus cloud spectra over water surfaces measured with the NASA/JPL AVIRIS instrument from an ER-2 aircraft at 20 km altitude. The bandpasses of a few MODIS channels are marked in thick horizontal bars. Because cirrus clouds are much higher than cumulus clouds, the peak absorption feature of the 0.94-μm water vapor band for the cirrus spectrum is much smaller than that for the cumulus spectrum.

In the presence of optically thick clouds, the 2-channel ratios (see Eq. (2)) provide information about absorptions due to water vapor molecules on the Sun-cloud-sensor path. The absorption effect is enhanced slightly due to multiple scattering of solar radiation within clouds. In order to infer the actual number of water vapor molecules that interacted with solar radiation, the cloud top height must be known, because molecular absorptions depend on atmospheric pressures. The cloud top heights for low level water clouds are difficult to determine accurately

from passive remote sensing data. Therefore, we plan to retrieve "effective" column water vapor amounts from the 2-channel ratio values from pixels with thick water clouds by assuming that the cloud top heights are at the sea level. These effective water vapor amounts can, in principle, be used to estimate the water vapor absorption effects in MODIS channels shorter than about 4 μm, provided that water vapor transmittances for different MODIS channels are calculated with the same assumption of cloud top heights being at the sea level. The cloud top heights for upper level thick cirrus clouds can be retrieved from MODIS IR emission channels (Menzel et al., 1991; King et al., 1992). From the 2-channel ratio values plus the estimated IR cloud heights, the column water vapor amount over thick cirrus pixels can be retrieved.

In the presence of optically thin clouds (usually ice clouds), an index on column water vapor amount above and within cirrus clouds can be established. Our recent analysis of AVIRIS data acquired over water surfaces indicates that the ratio of the radiance from the 0.94-μm channel against the radiance from the 0.865-μm channel provides information about water vapor above and within cirrus clouds. Because the water surface away from sun glint regions is black above 0.8 μm, it has no contribution to the 2-channel ratio. The sensitivities of MODIS IR channels near 14 μm are not sufficiently high for reliable detection of thin cirrus clouds with effective IR emissivities less than about 0.04. The estimation of the heights of such thin cirrus clouds using CO2 slicing techniques is certainly not possible. For slightly thicker cirrus clouds, the CO2-slicing technique can sometimes successively estimate the heights of such clouds, but often has a tendency to underestimate the height of such clouds due to intrinsic absorption, emission, and partial transparent nature of cirrus clouds. Based on these considerations, we have concluded that thin cirrus cloud heights will have to be assumed at a few discrete height levels based on climatology. From the 2-channel ratios and the assumed cirrus heights, the upper level water vapor index can be established.

3.1.2 Mathematical Description of the Algorithm

Atmospheric water vapor has very different absorption coefficients over the bandpasses of MODIS channels centered near 0.935, 0.940, and 0.905 μm. As a result, the three channels have different water vapor sensitivities under the same atmospheric condition. The strong absorption channel at 0.935 μm is most sensitive under dry conditions, while the weak absorption channel at 0.905 μm is most sensitive under humid conditions. Under a given atmospheric condition, the

derived water vapor values from the three channels can be different. A mean water vapor value (W) will be obtained according to the equation:

$$W = f_1 W_1 + f_2 W_2 + f_3 W_3 \quad (4)$$

where W_1, W_2, and W_3 are water vapor values from the 0.935, 0.940, and 0.915 μm channels, respectively, and f_1, f_2, and f_3 are the corresponding weighting functions. Our currently adopted weighting functions are based on the sensitivity of the transmission (T_i) in each of the channels (i) to the total precipitable water vapor (W): $\eta_i = |\Delta T_i / \Delta W|$. The weighting functions, f_i, are defined as the normalized values of η_i:

$$f_i = \eta_i / (\eta_1+\eta_2+\eta_3); \qquad \eta_i = |\Delta T_i / \Delta W| \quad (5)$$

These weighting functions are computed numerically from simulated curves of transmittances versus precipitable water. Figure 6 shows the dependence of f_i on the total precipitable water vapor for the three filters.

3.1.3 Descriptions of Input and Output Data

The Level 2 near-IR water vapor algorithm requires input data sets from standard MODIS data cubes and associated ancillary data. The inputs from MODIS data cubes are radiances from five MODIS channels centered at 0.865, 0.905, 0.936, 0.94, and 1.24 μm. The inputs from ancillary data are solar zenith angle, view zenith angle, relative azimuth angle between the solar and viewing directions, cloud mask, land-water flag, surface elevation, and surface temperature. The required angular information is for converting the total 2-way path water vapor amount to the vertical column amount. The cloud mask is used to indicate whether the pixel is clear or cloudy. The land-water flag is used to show if the pixel is over land or water. Both the cloud mask and land-water flag are used in our selection of either the 2-channel or the 3-channel ratio method in the retrievals. Because molecular absorption depends on pressure, surface elevations in digital form are used in our algorithm for pressure scaling of water vapor amounts (the same scheme as LOWTRAN7). Surface temperature is used in selection of the appropriate model atmosphere in the retrieval.

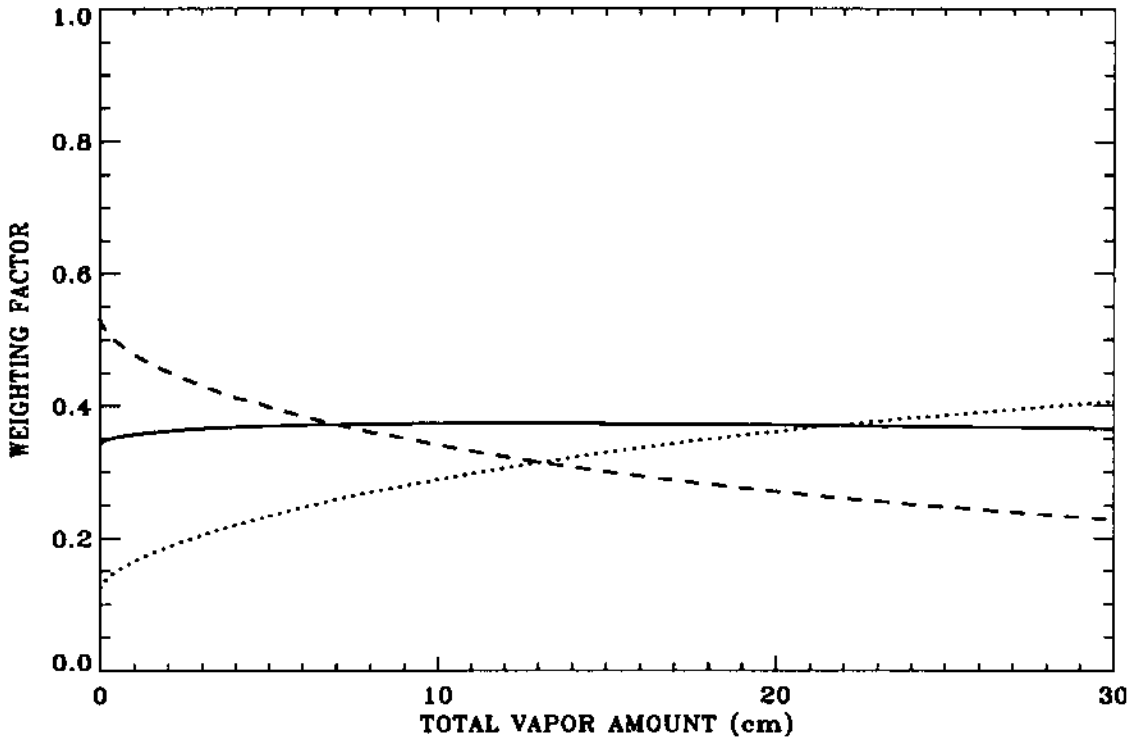

Fig. 6. The normalized weighting factors as a function of total precipitable water vapor. Solid line for the wide 0.94 μm channel, dashed line for the narrow 0.935 μm channel, and the dotted line for the 0.905 μm channel.

The output from the Level 2 near-IR water vapor algorithm includes column water vapor amounts on a pixel-by-pixel basis and an associated quality assurance parameter. The column water vapor amounts are derived over clear land areas of the globe, and above clouds over both land and ocean. Water vapor estimates are also made over extended glint oceanic area. The quality assurance parameter has been implemented in the Version 2 near-IR water vapor algorithm. In addition to the Level 2 near-IR water vapor product, Level 3 (MOD43) gridded products will be produced daily, 8-day, and monthly .

3.1.4 Variance or Uncertainty Estimates

Several sources of errors in column water vapor retrievals from MODIS channels have been described by Kaufman and Gao (1992) and summarized in Table IV of the paper. The sources of errors include:

1. Uncertainty in the spectral reflectance of the surface.
2. Uncertainty in the sensor calibration.
3. Effect of mixed pixels and clouds.
4. Effect of a shift in the channel location.
5. Uncertainty in pixel registration between several spectral channels.
6. Uncertainty in the atmospheric temperature and moisture profile.
7. Uncertainty in the amount of haze.

The largest sources of errors are the uncertainty in spectral reflectances of surface targets and the uncertainty in the amount of haze. Because channel ratios are used in the algorithm, only the relative channel-to-channel radiometric calibration is important. Spatial averaging can greatly alleviate the problem of mis-registration between channels. The overall water vapor error is expected to be 13%. If additional MODIS channels are used to infer the types of the surfaces and the amount of haze from MODIS data, the overall error can be reduced to about 7% at the expense of a more complex retrieval algorithm.

3.2 Practical Considerations

Considerations of numerical computation, programming, and exception handling are presented in this section.

3.2.1 Numerical Computation Considerations

Problems with numerical stability and round-off errors are not expected with this algorithm.

3.2.2 Programming/Procedural Considerations

The use of look-up table is the logical choice to speed up the retrieval processes. There is no need to perform direct radiative transfer modeling on a pixel-by-pixel

basis. The computational effort involved will be determined later, but it will essentially corresponds to 200 (or less) simple operations per pixel.

Because several MODIS products depend on the near-IR water vapor values for atmospheric corrections, we have decided to derive column water vapor values on a pixel-by-pixel basis. For the actual MODIS data, we do not expect major problems in producing the pixel-by-pixel-based water vapor images, because the spatial registrations for the five channels used in this algorithm are very good (within ~0.1 pixel).

3.2.3 Implementation of Aerosol Correction Module

We plan to correct for the aerosol effects in the Level 2 near-IR water vapor product. The effect of haze on remote sensing of water vapor depends on the amount of haze and the magnitude of the surface reflectances. Under typical atmospheric conditions with visibilities of 20 km or greater, the aerosol effects on water vapor retrievals are not significant. However, under hazy conditions (with visibilities less than 10 km) or when the surface reflectances near 1 μm are small (less than about 0.1), errors can be 10% or slightly greater in our retrieved water vapor values using the atmospheric transmittance model if the aerosol effects are not corrected. The application of our near-IR water vapor product with 10% errors will typically result in satisfactory corrections of water vapor effects in other "weakly absorbing" near-IR MODIS channels.

At present, a module for correcting aerosol effects has been developed and implemented in our near-IR water vapor algorithm. In this module, the Level 2 aerosol optical depth image and the water vapor image derived with the atmospheric transmittance model are read in. Scaling factors are derived using the aerosol optical depths and lookup table procedures. These scaling factors are then applied to the water vapor image to produce the final aerosol-effect-corrected water vapor image. Two pre-calculated lookup tables are used during the derivation of the scaling factors. One lookup table contains apparent reflectances of the 0.865-μm channel, which are functions of aerosol optical depth, column water vapor amount, surface reflectance, solar zenith angle, view zenith angle, and relative azimuth angle. The other lookup table contains apparent reflectances of the 0.94-μm channel. The lookup tables were generated using DISORT, a radiative transfer code developed by Stamnes et al. (1988). The k-distribution coefficients were used as inputs to DISORT in order to properly take care of water vapor effects. A rural aerosol model of Shettle and Fenn (1979) for a relative humidity of 70% was used.

The radiative transfer calculations were performed for 8 aerosol optical depths at 0.55 μm (0, 0.1, 0.25, 0.5, 1.0, 2.5, 3.5, and 5.0), 13 column water vapor amounts (0.1, 0.2, 0.4, 0.7, 1.0, 1.5, 2.0, 3.0, 4.0, 5.0, 7.0, 10.0, and 15.0 cm), 8 surface reflectance values at 0.865 μm (0.01, 0.03, 0.05, 0.1, 0.2, 0.4, 0.6, and 1.0), 10 solar zenith angles (0, 10, 20, 30, 40, 50, 60, 70, 75, and 80 degrees), 7 view zenith angles (0, 10, 20, 30, 40, 50, and 60 degrees), and 19 relative azimuth angles (0, 5, 10, 20, 30, 40, 60, 80, 90, 100, 110, 120, 130, 140, 150, 160, 170, 175, and 180 degrees). The selections of these grids were influenced by the work of Fraser et al. (1989) on the development of an atmospheric correction algorithm for processing Landsat and AVHRR images.

3.2.4 Exception Handling

The version 2 near-IR water vapor algorithm handles variable sizes of MODIS data cubes and day/night modes. It also handles input MODIS data with artifacts, such as missing lines, dead detectors, and missing packets.

3.2.5 Constraints and Limitations

Most of the constraints and limitations of the algorithm have already been described in Section 3.1.4.

4 Calibration, Validation, and Quality Assurance

The basic physics of using channels within and around the 0.94-μm water vapor band for column water retrievals is well understand. The solar radiation within the 0.94-μm water vapor band on the Sun-surface-sensor path is partially absorbed by atmospheric water vapor. The column water vapor amount is derived from this absorption signature. Previously, a 3-channel ratio technique (Kaufman and Gao, 1992), similar to the one implemented in the present version 2 of MODIS near-IR water vapor algorithm, was applied to a number of spectral imaging data sets measured with the NASA/JPL AVIRIS instrument from an ER-2 aircraft at 20 km. The derived column water vapor amounts agreed very well with water vapor measurements made with radiosondes and upward-looking microwave radiometers.

In order to derive accurately the column water vapor amounts from MODIS data, the transmission functions of MODIS filters centered near 0.86, 0.905, 0.935, 0.94, and 1.24 μm must be known precisely, particularly for the three water vapor absorption channels centered near 0.905, 0.935, and 0.94 μm. Errors in filter

transmission functions will result in systematic errors in derived column water vapor amounts, as one can expect from the water vapor transmission spectra in Fig. 1. Fortunately, the MODIS instrument provides onboard monitoring capability of the required transmission functions.

Before the launch of the MODIS instrument into space, we plan to further test the near-IR water vapor algorithm using spectral imaging data collected by AVIRIS and the MODIS Airborne Simulator (MAS) during several field experiments, including the SCAR-A (Sulfates, Clouds, And Radiation - Atlantic) experiment conducted over the eastern coastal areas of the United States in July of 1993 and the SCAR-B (Smoke, Clouds, And Radiation - Brazil) experiment conducted in September of 1995 over Brazil.

In addition to airborne MAS and AVIRIS observations, AERONET (AErosol RObot NETwork) sunphotometers also provide water vapor observations from the ground, which can also be used to test the algorithm. The sunphotometer measures the absorption of water vapor at 0.94 μm. By subtracting aerosol scattering effect from adjacent channels and molecular scattering, the total precipitable water vapor amounts are derived using modified Langley method (Reagan et al., 1987). As found, errors in derived precipitable water ranged from 5 to 15% when compared to in-situ measurements with radiosondes and ground-based microwave radiometers for variable water vapor amounts between 1 and 5 cm at locations from high latitude boreal forest to tropical rain forest and from urban area to desert (Halthore et al., 1996; Holben and Eck, 1990). Seasonal variation is also clearly seen from wet to dry season at Sahel, west Africa owing to the movement of ITCZ (Inter-Tropical Convergence Zone), and in the rain forest in Brazil from summer to winter. Much of the results are from BOREAS (BOReal Ecosystem Atmospheric Study) field campaign in North-central Canada, and earlier established stations for the purpose of measuring different types of aerosols world wide. In the last three years, AERONET sunphotometer deployments have played an important role in a series of SCAR field experiments. Because of easy maintenance and good calibration, and central network communication capability, there are plans to expand AERONET as part of international research and monitoring activities, and as part of the support and validation of analysis for future satellite systems. Therefore, the sunphotometer water vapor measurements should provide results with sufficiently wide coverage and good accuracy, which can be used to validate the total precipitable water vapor amounts derived from MODIS.

We plan to implement a quality control parameter to indicate the reliability of the retrievals. For high reflecting land surfaces, the signal to noise ratios of data from the five MODIS channels are expected to be 100 or greater, and the reliability of the retrieved water vapor values is expected to be high. The reverse is true for the low reflecting water surfaces.

After the launch of the MODIS instrument into space, we plan to participate in several field campaigns. Using in-situ and remote sensing data from field campaigns, we will validate the retrieved water vapor values from MODIS data. Specifically, the water vapor values retrieved from MODIS data will be compared with those from AVIRIS and MAS data, from in situ radiosonde measurements, ground-based upward looking microwave radiometers (such as those located at DOE ARM sites), the AERONET sunphotometers, and Raman lidar (Melfi et al., 1989). We are also interested in comparing the MODIS near-IR water vapor images with those obtained from the Japanese Global Positioning System/Meteorological Project (GPS/MET). Japan has deployed a GPS array and currently operates about 1000 stations with a mean separation of about 15-30 km (Naito et al., 1998).

The quality control will be performed in two dimensions. The first is analysis using specific sites in different climatic and geographic regions where validation data are available. The second is statistical analysis of the whole data set. For both analyses the total precipitable water vapor values will be examined to see if a systematic dependence on viewing direction exists. Presence of negative numbers will be indicated. The quality of the data from a specific validation site will be correlated to the reflectance properties of the site.

5 Research Agenda

Under unusual circumstances, such as after the eruption of a major volcano, the stratospheric aerosol concentrations can be very high. For example, soon after the eruption of the Mt. Pinatubo volcano in the summer of 1991, the stratospheric aerosol optical depths in the visible part of the spectrum were 0.2 or greater. These stratospheric aerosols can scatter solar radiation into the field-of-view of the MODIS instrument. The amount of path scattered solar radiance near 1 μm due to stratospheric aerosols can be non-negligible, particularly over dark surfaces. The path radiances near 0.94 and 1.38 μm contain essentially no water vapor absorption effects because of high altitudes of stratospheric aerosol layers. These path radiances need to be subtracted out from the total MODIS observed radiances before normal retrievals of column water vapor amounts can be made. Therefore, techniques for

estimating the stratospheric aerosol path radiances need to be developed. The wavelength dependencies of path radiances due to scattering by atmospheric molecules (Rayleigh scattering), cirrus clouds, and stratospheric aerosols are very different. We anticipate scatter plots, such as those of 0.86-µm versus 0.94-µm, 0.86-µm versus 1.24-µm, and 0.86-µm versus 1.375-µm, will yield information on the path radiances resulting from stratospheric aerosol scattering.

6 References

Asrar, G., R. Greenstone, (Editors), Mission to planet earth / earth observing system reference handbook, National Aeronautics and Space Administration, Goddard Space Flight Center, Mail Code 900, Greenbelt, MD 20771, USA, 277p., 1995.

Bowker, D. E., R. E. Davis, D. L. Myrick, K. Stacy, and W. T. Jones, Spectral reflectances of natural targets for use in remote sensing studies, *NASA Ref. Publ. 1139*, 1985.

Chesters, D. C., L. W. Uccellini, and W. D. Robinson, Low-level water vapor fields from the VISSR Atmospheric Sounder (VAS) "split-window" channels, *J. Clim. Appl. Meteor.*, 22, 725-743, 1983.

Condit, H. R., The spectral reflectance of American soils, *Photogramm. Eng., 36,* 955–965, 1970.

Fraser, R. S., R. A. Ferrare, Y. J. Kaufman, and S. Mattoo: Algorithm for atmospheric corrections of aircraft and satellite imagery, pp. 1-98, *NASA Technical Memorandum 100751*, 1989, Washington, DC

Fraser, R. S. and Y. J. Kaufman, The relative importance of aerosol scattering and absorption in remote sensing, *IEEE J. Geosc. Rem. Sens.*, GE-23, 525-633, 1985.

Gao, B. C., and Alexander F. H. Goetz, Column Atmospheric Water Vapor and Vegetation Liquid Water Retrievals From Airborne Imaging Spectrometer Data, *J. Geophys. Res., 95,* 3549-3564, 1990.

Gao, B.-C., K. B. Heidebrecht, and A. F. H. Goetz, Derivation of scaled surface reflectances from AVIRIS data, *Remote Sens. Env.*, 44, 165-178, 1993.

Hansen, J. E. and L. D. Travis, Light scattering in planetary atmospheres. *Space Science Reviews*, 16, 527-610, 1974.

Halthore, R., T. F. Eck, B. N. Holben, and B. L. Markham, 1996: Sunphotometric measurements of atmospheric water vapor column abundance in the 940-nm band, accepted by J. Geophys. Res., 1996.

Holben, B. N. and T. F. Eck, 1990: Precipitable water in the Sahel measured using sunphotometry, *Agricultural and Forest Meteorology, 52,* 95-107.

Kaufman, Y. J., and B.-C. Gao, Remote sensing of water vapor in the near IR from EOS / MODIS, *IEEE Trans. Geosci. Remote Sensing,*, 30, 871-884, 1992.

King, M. D., Y. J. Kaufman, W. P. Menzel, and D. Tanre, Remote sensing of cloud, aerosol, and water vapor properties from the Moderate Resolution Imaging Spectrometer (MODIS), *IEEE Trans. Geosci. Remote Sensing,*, 30, 1-27, 1992.

Kneizys, F. X., E. P. Shettle, L. W. Abreu, J. H. Chetwynd, G. P. Anderson, W. O. Gallery, J. E. A. Selby, and S. A. Clough, Users guide to LOWTRAN 7, AFGL–TR–8–0177, Air Force Geophys. Lab., Bedford, Mass., 1988.

Melfi, S. H., D. Whiteman, and R. Ferrare, Observation of atmospheric fronts using Raman lidar moisture measurements, J. Appl. Meteorol., 28, 789-806, 1989

Menzel, W. P., D. P. Wylie, and K. I. Strabala, Seasonal and diurnal changes in cirrus clouds as seen in four years of observations with the VAS, *J. Appl. Meteorol.*, 31,370-385, 1992.

Naito, I., Y. Hatanaka, N. Mannoji, R. Ichikawa, S. Shimada, T. Yabuki, H. Tsuji, and T. Tanaka: Global positioning system project to improve Japanese weather, earthquake predictions, *EOS Transa. Amer. Geophys. Union, 79*, 301, 1998.

Salomonson, V. V., et al., MODIS: Advanced facility instrument for studies of the Earth as a system, *IEEE Trans. Geosci. Remote Sens., 27*, 145, 1989.

Shettle, E. P., and R. W. Fenn: Models for the aerosols of the lower atmosphere and the effects of humidity variations on their optical properties., AFGL-TR-79-0214, Air Force Geophys. Lab, Hanscom AFB, MA.

Stamnes, K., S.-C. Tsay, W. Wiscombe, and K. Jayaweera: Numerically stable algorithm for discrete-ordinate-method radiative transfer in multiple scattering and emitting layered media, *Appl. Opt., 27, 2502-2509*, 1988.

Stoner, E. R., and M. F. Baumgardner, Physiochemical, site and bidirectional reflectance factor characteristics of uniformly moist soils, pp. 1–50, *NASA CR-160571*, 1980.

Susskind, J., J. Rosenfield, and D. Reuter, Remote sensing of weather and climate parameters from HIRS2/MSU on TIROS-N, *J. Geophys. Res.*, 89, 4677-4697, 1984.

Vane, G., R. O. Green, T. G. Chrien, H. T. Enmark, E. G. Hansen, and W. M. Porter, The Airborne Visible/Infrared Imaging Spectrometer, *Remote Sens. Env., 44*, 127-143, 1993.

APPENDIX A

A reprint of the paper, *Remote Sensing of Water Vapor in the Near IR from EOS/MODIS*, by Kaufman and Gao (1992).

APPENDIX B

A reprint of the paper, *Column Atmospheric Water Vapor and Vegetation Liquid Water Retrievals From Airborne Imaging Spectrometer Data*, by Gao and Goetz (1990).